

Effective pair gap of weakly bound neutrons in deformed nuclei

Ikuko Hamamoto^{1,2}

¹*Division of Mathematical Physics, Lund Institute of Technology at the University of Lund, Lund, Sweden*

²*The Niels Bohr Institute, Blegdamsvej 17, Copenhagen Ø, DK-2100, Denmark*

(Received 2 November 2004; published 9 March 2005)

The dependence of effective pair gap on weakly bound neutron orbits is studied in deformed nuclei in comparison with that in spherical nuclei, solving the Hartree-Fock-Bogoliubov equation in a simplified model in coordinate space with the correct asymptotic boundary conditions. In spherical nuclei the effective pair gap of $s_{1/2}$ neutrons decreases to zero in the limit that the corresponding Hartree-Fock one-particle energy approaches zero. In the same limit, the effective pair gap of $\Omega^\pi = 1/2^+$ neutrons in deformed nuclei becomes very small when the wave functions of $\Omega^\pi = 1/2^+$ orbits contain an appreciable amount of $s_{1/2}$ components, even if a considerable amount of larger- ℓ components remains in the wave functions. Then, the one-particle excitation spectra of deformed even-even neutron-drip-line nuclei, in which an $\Omega^\pi = 1/2^+$ level is weakly bound, can start at much lower energy than twice the average pair gap in the presence of many-body pair correlation.

DOI: 10.1103/PhysRevC.71.037302

PACS number(s): 21.60.Ev, 21.10.Pc, 21.60.Jz

The physics of nuclei far from the β -stability line, especially close to the neutron drip line, issues an intensive challenge to the conventional theory of nuclear structure. A feature unique to the weakly bound neutron systems is the importance of the coupling to the nearby continuum of unbound states, as well as the impressive role played by weakly bound neutrons with small orbital angular momentum ℓ . Because the Fermi level of drip line nuclei in the mean-field approximation lies very close to the continuum, the many-body correlations in the ground state such as deformation or pair correlation necessarily receive significant contributions by some of an infinite number of one-particle levels which in the mean-field approximation lie in the continuum. Weakly bound small- ℓ neutrons have an appreciable probability to be outside of the core nucleus and are thereby insensitive to the strength of the one-body potential provided by the well-bound nucleons in the system, whereas the wave functions of weakly bound large- ℓ neutrons stay mostly inside the nuclear potential.

Using a simplified model in the Hartree-Fock-Bogoliubov (HFB) approximation, in Ref. [1] the unique role of neutron lower- ℓ orbits in the pair correlation of spherical nuclei close to the neutron drip line is studied in detail, whereas the possible appearance of broad low-energy spin response in some spherical neutron-drip-line nuclei with many-body pair correlations is pointed out in Ref. [2]. On the other hand, in Ref. [3] the unique behavior of those neutrons in deformed neutron-drip-line nuclei is described in the absence of the pair correlation. Combining the results of Refs. [1,3], it is conjectured that in deformed nuclei all $\Omega^\pi = 1/2^+$ levels become practically unavailable for both deformation and many-body pair correlation, when in the mean-field

approximation the levels approach continuum or lie in the continuum. In this article we extend the simplified HFB model to the one that includes both deformation and many-body pair correlation, solving the HFB equation in coordinate space with the correct asymptotic boundary conditions. In particular, the dependence of effective pair gap on neutron orbits in deformed nuclei is studied.

We consider the time-reversal invariant and axially symmetric quadrupole-deformed system with many-body pair correlation. We follow the HFB formalism of Refs. [4,5], which is formulated for spherical nuclei in coordinate space with correct boundary conditions, and extend it to deformed nuclei with many-body pair correlation. We write single-quasiparticle wave functions as follows:

$$\Psi_{\ell j \Omega}^i(\vec{r}) = \sum_{\ell j} R_{\ell j \Omega}^i(E_{qp}, r) \mathbf{Y}_{\ell j \Omega}(\hat{r}), \quad i = 1, 2, \quad (1)$$

where Ω expresses the component of one-particle angular momentum \vec{j} along the symmetry axis, which is a good quantum number, and

$$\mathbf{Y}_{\ell j \Omega}(\hat{r}) \equiv \sum_{m_\ell, m_s} C\left(\ell, \frac{1}{2}, j; m_\ell, m_s, \Omega\right) Y_{\ell m_\ell}(\hat{r}) \chi_{m_s}. \quad (2)$$

The upper ($i = 1$) and lower ($i = 2$) components of the radial wave functions are introduced as follows:

$$r R_{\ell j \Omega}^i(E_{qp}, r) = u_{\ell j \Omega}(E_{qp}, r) \quad \text{and} \quad v_{\ell j \Omega}(E_{qp}, r). \quad (3)$$

Assuming that both the Hartree-Fock (HF) and pair potentials are given by the well-bound core nucleus, our HFB equation is reduced to the coupled equations for $u_{\ell j \Omega}$ and $v_{\ell j \Omega}$, which are written as follows:

$$\left. \begin{aligned} & \left(\frac{d^2}{dr^2} - \frac{\ell(\ell+1)}{r^2} + \frac{2m}{\hbar^2} (\lambda + E_{qp}^\Omega - V(r) - V_{so}(r)) \right) u_{\ell j \Omega}(r) - \frac{2m}{\hbar^2} \Delta_0(r) v_{\ell j \Omega}(r) \\ & = \frac{2m}{\hbar^2} \sum_{\ell' j'} \langle \mathbf{Y}_{\ell j \Omega} | V_{\text{coupl}} | \mathbf{Y}_{\ell' j' \Omega} \rangle u_{\ell' j' \Omega}(r) + \frac{2m}{\hbar^2} \sum_{\ell' j'} \langle \mathbf{Y}_{\ell j \Omega} | \Delta_{20} | \mathbf{Y}_{\ell' j' \Omega} \rangle v_{\ell' j' \Omega}(r), \\ & \left(\frac{d^2}{dr^2} - \frac{\ell(\ell+1)}{r^2} + \frac{2m}{\hbar^2} (\lambda - E_{qp}^\Omega - V(r) - V_{so}(r)) \right) v_{\ell j \Omega}(r) + \frac{2m}{\hbar^2} \Delta_0(r) u_{\ell j \Omega}(r) \\ & = \frac{2m}{\hbar^2} \sum_{\ell' j'} \langle \mathbf{Y}_{\ell j \Omega} | V_{\text{coupl}} | \mathbf{Y}_{\ell' j' \Omega} \rangle v_{\ell' j' \Omega}(r) - \frac{2m}{\hbar^2} \sum_{\ell' j'} \langle \mathbf{Y}_{\ell j \Omega} | \Delta_{20} | \mathbf{Y}_{\ell' j' \Omega} \rangle u_{\ell' j' \Omega}(r), \end{aligned} \right\} \quad (4)$$

We use the Woods-Saxon potential as a replacement of the HF potential and have included only the lowest-order term in deformation parameter β of both the deformed Woods-Saxon and deformed pairing potentials. This is an approximation; however, for our present purpose to illustrate the unique behavior of weakly bound neutrons with small Ω values the simple form of the deformed potential is sufficient. The quantities appearing in Eq. (4) are as follows:

$$\begin{aligned}
V(r) &= V_{WS} f(r), \\
V_{\text{coupl}}(\vec{r}) &= -\beta k(r) Y_{20}(\hat{r}), \\
V_{so}(r) &= -V_{WS} v \left(\frac{\Lambda}{2} \right)^2 \frac{1}{r} \frac{df(r)}{dr} (\vec{\sigma} \cdot \vec{\ell}), \\
\langle \mathbf{Y}_{\ell j \Omega} | V_{\text{coupl}} | \mathbf{Y}_{\ell' j' \Omega} \rangle &= -\beta k(r) \langle \mathbf{Y}_{\ell j \Omega} | Y_{20}(\hat{r}) | \mathbf{Y}_{\ell' j' \Omega} \rangle \\
&= -\beta k(r) (-1)^{\Omega-1/2} \\
&\quad \times \sqrt{\frac{(2j+1)(2j'+1)}{20\pi}} \\
&\quad \times C(j, j', 2; \Omega, -\Omega, 0) \\
&\quad \times C(j, j', 2; \frac{1}{2}, -\frac{1}{2}, 0), \tag{5}
\end{aligned}$$

where Λ is the reduced Compton wavelength of nucleon $\hbar/m_r c$,

$$f(r) = \frac{1}{1 + \exp\left(\frac{r-R}{a}\right)} \tag{6}$$

and

$$k(r) = RV_{WS} \frac{df(r)}{dr}. \tag{7}$$

The matrix elements of Δ_{20} in Eq. (4) are obtained from those of V_{coupl} in Eq. (5) by replacing $V_{WS}(df(r)/dr)$ with $d\Delta_0(r)/dr$. We fix the parameters to be $a = 0.67$ fm, $V_{WS} = -51$ MeV, and $v = 32$, which are the standard parameters used in β stable nuclei [6]. The strength of the one-body potential is varied by changing the radius of the potential R in units of $r_0 = 1.27$ fm. The monopole pairing field is taken to be local as a function of radius parameter. We have tried the functional form of either the volume-type pairing, $\Delta_0(r) \propto f(r)$, or the surface-type pairing, $\Delta_0(r) \propto r \frac{df(r)}{dr}$. The averaged strength of the pair field defined by the following:

$$\bar{\Delta} \equiv \frac{\int_0^\infty r^2 dr \Delta_0(r) f(r)}{\int_0^\infty r^2 dr f(r)} \tag{8}$$

is an input of numerical calculations expressing the strength of the pair field.

In numerical integrations we use a radial mesh $\Delta r = 0.025$ fm in the neighborhood of the origin $r=0$, whereas $\Delta r = 0.2$ fm is used otherwise. The radial integration is carried out to $r_{\text{max}} = 70$ fm. The way of solving the coupled Eq. (4) is taken from Ref. [7].

In the present work we restrict ourselves to the discrete eigenvalue problem of Eq. (4) where $(\lambda + E_{qp}^\Omega) < 0$, in which the asymptotic behavior of HFB wave functions for $r \rightarrow \infty$ is as follows:

$$\begin{cases} u_{\ell j \Omega}(E_{qp}^\Omega, r) \propto r h_\ell(\alpha_u r) \\ v_{\ell j \Omega}(E_{qp}^\Omega, r) \propto r h_\ell(\alpha_v r) \end{cases} \tag{9}$$

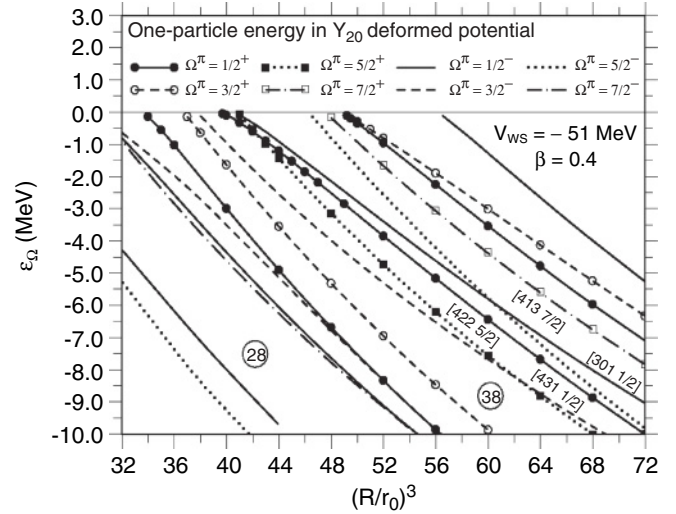


FIG. 1. Neutron one-particle energies in axially symmetric quadrupole-deformed Woods-Saxon potentials as a function of the potential strength. The radius of the Woods-Saxon potential is expressed by R , whereas $r_0 = 1.27$ fm is used. The asymptotic quantum numbers $[N n_z \Lambda \Omega]$ traditionally assigned are indicated for the [422 5/2], [431 1/2], [301 1/2], and [413 7/2] levels, where only Ω and $\pi = (-1)^N$ are good quantum numbers. The neutron numbers 28 and 38, which are obtained by filling in all lower lying levels, are represented with circles.

where $h_\ell(-iz) \equiv j_\ell(z) + in_\ell(z)$, in which j_ℓ and n_ℓ are spherical Bessel and Neumann functions, respectively, and

$$\begin{cases} \alpha_u^2 \equiv -\frac{2m}{\hbar^2} (\lambda + E_{qp}^\Omega) \\ \alpha_v^2 \equiv -\frac{2m}{\hbar^2} (\lambda - E_{qp}^\Omega) \end{cases} \tag{10}$$

The normalization of the wave functions is written as follows:

$$\sum_{\ell j} \int_0^\infty (|u_{\ell j \Omega}(E_{qp}^\Omega, r)|^2 + |v_{\ell j \Omega}(E_{qp}^\Omega, r)|^2) dr = 1. \tag{11}$$

First we show some quantities calculated for the neutron numbers of our present interests in the absence of pair correlation, which were basically studied in Ref. [3]. In Fig. 1 we show neutron one-particle energies calculated in the absence of pair field as a function of the potential strength for $\beta = 0.4$ and the neutron number $N \approx 28 - 54$, where the $3s_{1/2}$ component may play a role for weakly bound deformed orbits with $\Omega^\pi = 1/2^+$. The asymptotic quantum numbers $[N n_z \Lambda \Omega]$ are written for four orbits, which are used in Fig. 3. In Fig. 2 the calculated components in the wave function of the [431 1/2] level are plotted as a function of the energy ε_Ω , which is the one-particle eigenenergy of the deformed Woods-Saxon potential with no pair field. In the limit of $\varepsilon_\Omega \rightarrow 0$ the wave functions of $\Omega^\pi = 1/2^+$ orbits will become an $s_{1/2}$ wave function [3]: this fact was pointed out also in Ref. [8] using a finite square-well potential.

It is seen that in the entire range of ε_Ω plotted in Fig. 1 the slopes of the [413 7/2] and [422 5/2] levels are appreciably larger than those of the [431 1/2] and [301 1/2] levels. The largeness comes from the fact that the major components of both [413 7/2] and [422 5/2] levels have large ℓ

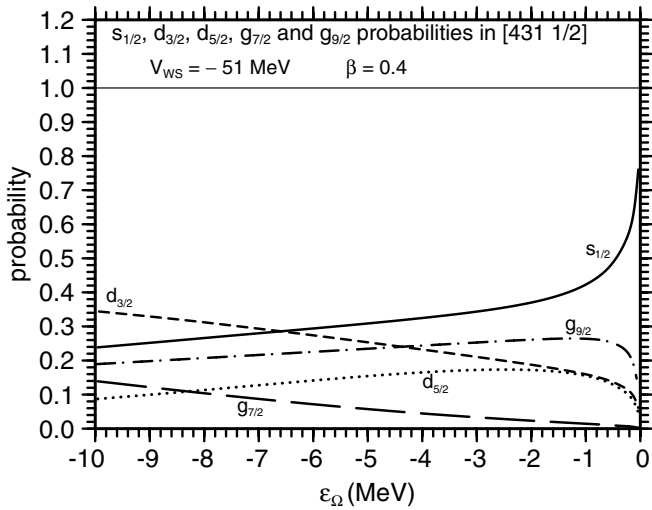


FIG. 2. Calculated components of the [431 1/2] level as a function of the energy eigenvalue ϵ_Ω of the deformed Woods-Saxon potential.

values: namely more than 86% of the [422 5/2] level comes from the $\ell \geq 4$ orbits, whereas the smallest ℓ component in the [413 7/2] level has $\ell = 4$. Conversely, the $\ell = 1$ components in the [301 1/2] level are always larger than 70%. Though it is known [9] that for $\beta = 0.4$ the structure of most one-particle levels can be approximately expressed by asymptotic quantum numbers and remains the same in the well-bound levels, say $\epsilon_\Omega \lesssim -5$ MeV, the present [431 1/2] level is one of exceptional cases as seen in Fig. 2, varying continuously the structure as a function of ϵ_Ω .

We define the effective pair gap Δ_{eff} by the following:

$$\Delta_{\text{eff}}^\Omega \equiv \min(E_{qp}^\Omega). \quad (12)$$

For a given potential strength the minimum value of E_{qp}^Ω on the r.h.s. of Eq. (12) is looked for, either taking the Fermi level

λ satisfying $\lambda = \epsilon_\Omega$ [2], where ϵ_Ω is a one-particle eigenvalue of the same deformed potential in the absence of pair field, or imposing the condition that the occupied and unoccupied probabilities of the level are equal to 0.5. These two conditions give in practice the same value of $\Delta_{\text{eff}}^\Omega$. In Fig. 3 the effective pair gap for four deformed one-particle orbits calculated with the Y_{00} pairing only is plotted as a function of the Fermi level λ thus obtained, taking the volume pairing $\bar{\Delta} = 1$ MeV. In axially symmetric deformed nuclei around the stability line it has been recognized that in most observable quantities the inclusion of Y_{20} pairing in addition to the Y_{00} pairing can be well approximated by renormalizing the strength of the Y_{00} pairing. Furthermore, this simple form of pairing may be justified by the fact that the analysis of the fingerprints of experimental data on deformed rare-earth nuclei is in a quantitative agreement with the theoretical estimate [9], which includes the Y_{00} pairing only. Here in Fig. 3 we mostly show Δ_{eff} values calculated only with the Y_{00} pairing, mainly because we want to compare the result for $\beta \neq 0$ with that for $\beta = 0$ in Fig. 4. However, for reference, in Fig. 3 we include the solid curve without symbols, which expresses Δ_{eff} values calculated for the [431 1/2] orbit, including the Y_{20} pairing, namely the Δ_{20} terms in Eq. (4) on top of the Y_{00} pairing without renormalizing the total strength. Because the [431 1/2] orbit strongly favors prolate deformation, the inclusion of the Y_{20} pairing makes a nearly λ -independent increase of Δ_{eff} by about 15%. Conversely, for example, the Y_{20} pairing makes an almost λ -independent decrease by about 5% for the [413 7/2] orbit, which moderately disfavors prolate deformation. Thus, we may conclude that the effect of including the Y_{20} pairing in addition to the Y_{00} pairing on respective Δ_{eff} values can well be simulated by a λ -independent renormalization of the strength of the Y_{00} pairing. In any case, the strong decrease of Δ_{eff} for the [431 1/2] orbit as $|\lambda| \rightarrow 0$ is obtained both with and without the Y_{20} pairing.

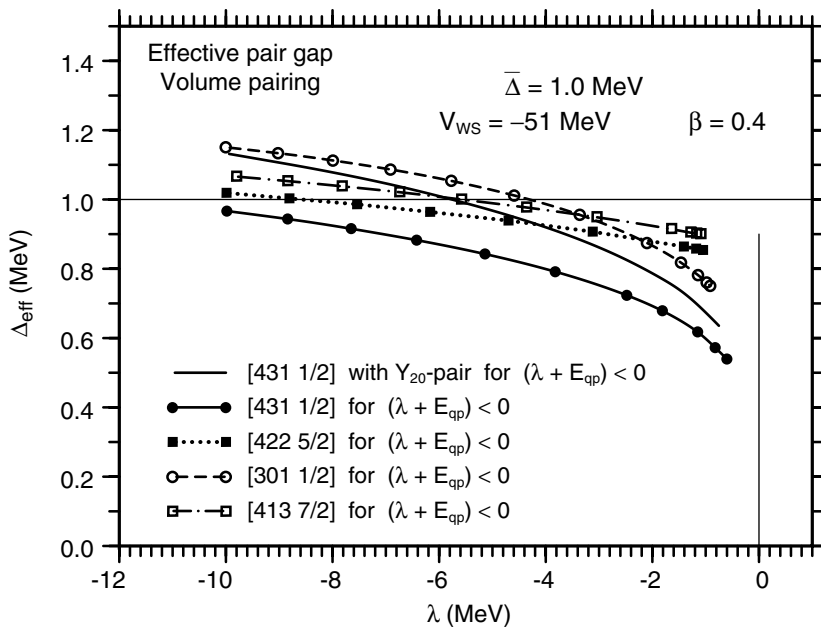


FIG. 3. Effective pair gap [Eq. (12)] of several deformed one-particle orbits as a function of the Fermi level λ , taking the quadrupole deformation $\beta = 0.4$ and $\bar{\Delta} = 1$ MeV. The curves with symbols show the Δ_{eff} values estimated by including the Y_{00} pairing only, whereas the solid curve without filled circles is calculated for the [431 1/2] orbit, including the Y_{20} pairing on top of the Y_{00} pairing without renormalizing the total strengths. See the text for details.

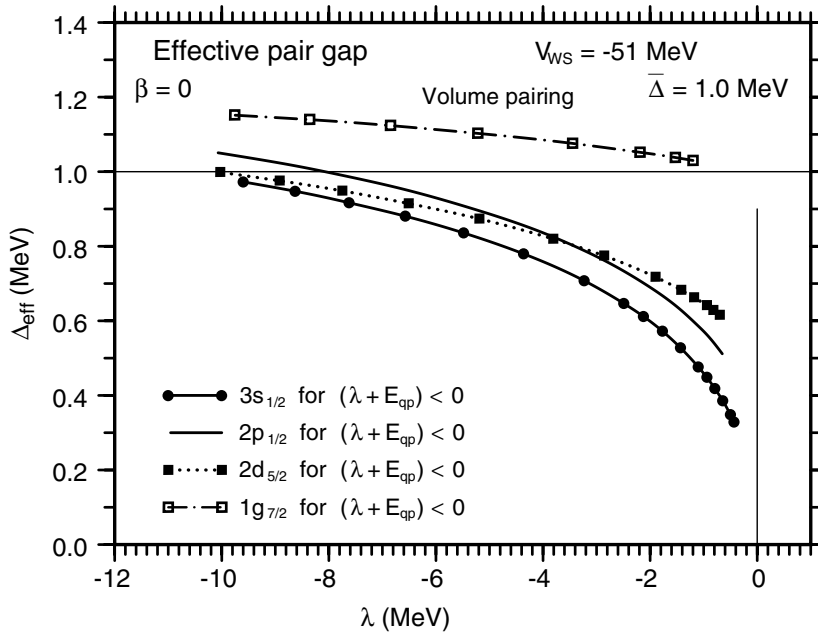


FIG. 4. Effective pair gap in the case of spherical nuclei as a function the Fermi level λ . Δ_{eff} is defined as the minimum value of $E_{qp}(\ell j)$, analogous to Eq. (12) in the case of deformed nuclei: For a given potential strength where $V_{WS} = -51$ MeV is fixed while R is varied, the minimum value of $E_{qp}(\ell j)$ is looked for and plotted as a function of λ .

For comparison, in Fig. 4 the corresponding quantity for spherical orbits is shown. The qualitative feature in Fig. 4 remains the same when we use the surface-type instead of the volume-type pairing, except that the curve for the $1g_{7/2}$ orbit slightly increases instead of decreasing as λ increases, because the $1g_{7/2}$ radial wave function has a slightly better overlap with the surface-type pair field for $\lambda \rightarrow 0$. Curves in Figs. 3 and 4 are plotted up to the maximum value of λ , at which the condition $(\lambda + E_{qp}) < 0$ is satisfied. At a certain finite value of $\lambda < 0$, which depends on the pair field $\Delta_0(r)$, one encounters $(\lambda + E_{qp}) = 0$ even for $s_{1/2}$ orbits. For $(\lambda + E_{qp}) > 0$ the HFB equation is not a discrete eigenvalue problem and, thus, the effective pair gap cannot be meaningfully defined as in Eq. (12). For larger ℓ orbits in spherical nuclei the condition $(\lambda + E_{qp}) = 0$ is fulfilled at larger values of $|\lambda|$, because the minimum values of E_{qp} at a given small value of $|\lambda|$ are larger for larger ℓ values. Extrapolating the curves in Fig. 4, it is easily seen that in the limit of $\lambda \rightarrow 0$ Δ_{eff} for the $s_{1/2}$ orbit decreases to zero, whereas Δ_{eff} for $\ell \neq 0$ orbits would be a finite value, which increases as ℓ increases. This ℓ dependence of the Δ_{eff} value in the limit of $\lambda \rightarrow 0$ can be qualitatively understood by noticing the following: In a finite square-well potential the probability of the one-particle wave function with

orbital angular momentum $\ell (\neq 0)$ staying inside the potential is equal to $(2\ell - 1)/(2\ell + 1)$ in the limit of zero binding energy, whereas the probability is zero for $\ell = 0$ orbits. See, for example, Chapter 3 of Ref. [6]. From Fig. 4 we conclude that the one-particle excitation spectra of spherical even-even neutron-drip-line nuclei, in which lower ℓ one-particle orbits are weakly bound, would start at much lower energy than $2\bar{\Delta}$.

Noting in Fig. 2 that for $\varepsilon_{\Omega} < -0.5$ MeV the $s_{1/2}$ component in the $[431\ 1/2]$ orbit is never larger than 50%, whereas the remaining components are those with $\ell = 2$ and 4, it is somewhat surprising to observe in Fig. 3 that Δ_{eff} decreases strongly as λ approaches zero. It seems that the magnitude of Δ_{eff} for weakly bound deformed one-particle orbits is not governed by the largest ℓ value with an appreciable component in the wave function but it is influenced considerably by the component with the smallest ℓ value. This observation indicates that the one-particle excitation spectra of deformed even-even neutron-drip-line nuclei, in which an $\Omega^{\pi} = 1/2^{+}$ level is weakly bound and thereby mostly decoupled from the many-body pair field, may start at much lower energy than $2\bar{\Delta}$, whereas well-bound core particles have a strong many-body pair correlation.

- [1] I. Hamamoto and B. R. Mottelson, Phys. Rev. C **68**, 034312 (2003); **69**, 064302 (2004).
 [2] I. Hamamoto and H. Sagawa, Phys. Rev. C **70**, 034317 (2004).
 [3] I. Hamamoto, Phys. Rev. C **69**, 041306 (2004).
 [4] A. Bulgac, preprint No. FT-194-1980, Institute of Atomic Physics, Bucharest, 1980, nucl-th/9907088.
 [5] M. Grasso, N. Sandulescu, Nguyen Van Giai, and R. J. Liotta, Phys. Rev. C **64**, 064321 (2001).

- [6] A. Bohr and B. R. Mottelson, *Nuclear Structure* (Benjamin, Reading, MA, 1969), Vol. I.
 [7] T. Tamura, Oak Ridge National Laboratory, Report ORNL-4152, 1967 (unpublished).
 [8] T. Misu, W. Nazarewicz, and S. Åberg, Nucl. Phys. **A614**, 44 (1997).
 [9] A. Bohr and B. R. Mottelson, *Nuclear Structure* (Benjamin, Reading, MA, 1975), Vol. II.